ELSEVIER

Journal of Immunological Methods 213 (1998) 41–52

JOURNAL OF IMMUNOLOGICAL METHODS

Rapid fluorescence-based measurement of neutrophil migration in vitro

C.W. Frevert [a,*], V.A. Wong [a], R.B. Goodman [a], R. Goodwin [b], T.R. Martin [a]

[a] *Medical Research Service of the Seattle VA Medical Center, Division of Pulmonary and Critical Care Medicine, Department of Medicine, University of Washington School of Medicine, Seattle, WA, USA*
[b] *Neuro Probe, Gaithersburg, MD, USA*

Received 25 August 1997; revised 9 January 1998; accepted 15 January 1998

Abstract

We have standardized a new chemotaxis chamber that uses fluorescence as the cellular marker for the measurement of leukocyte migration in vitro in disposable 96-well microplates. This new fluorescence-based assay is a robust assay because filter pore size, cell density, filter composition, and filter thickness do not affect PMN migration towards interleukin-8 or the complement fragment, C5a. When compared to two separate chemotaxis assays in which the migrated cells are counted visually, the fluorescence-based assay was more rapid, less labor intensive, and more sensitive. This new assay is a significant advance in the measurement of leukocyte migration in vitro.

Keywords: Leukocyte; Neutrophil; Migration; Chemotaxis; Interleukin-8; C5a; Fluorescence; Calcein AM

1. Introduction

Leukocyte migration is essential for leukocyte accumulation at sites of inflammation. In order to determine the mechanisms responsible for migration in vivo, leukocyte chemotaxis has been studied in vitro since 1917. Techniques that have been used to study leukocyte chemotaxis in vitro include methods in which chemotaxis is measured by direct observation of cellular migration, and methods in which chemotaxis is measured by quantifying leukocyte migration into or across membranes.

Methods used for the direct viewing of leukocyte chemotaxis include the application of cells to specialized slides and coverslips to visualize the orientation of leukocytes in gradients of chemotactic factors (e.g., Zigmond chamber) (Zicha et al., 1991; Zigmond, 1977). Other direct visual techniques include leukocyte chemotaxis under agarose (Krauss et al., 1994) and leukocyte chemotaxis in three dimensional-matrices of collagen (Haddox et al., 1994).

* Corresponding author. Seattle VAMC Pulmonary Research Group, Seattle VA Medical Center, 151L 1660 S. Columbian Way, Seattle, WA 98108, USA. Tel.: +1-206-764-2219; fax: +1-206-768-5289; e-mail: cfrevert@u.washington.edu.

0022-1759/98/$19.00
PII S0022-1759(98)00016-7

Boyden first described the use of membrane filters to study leukocyte chemotaxis in vitro in 1962 (Haddox et al., 1994). Membrane filters offered an important advantage for the study of leukocyte chemotaxis because they provided quantitative data. Several different methods have been used to measure leukocyte chemotaxis with membrane filters. These include a multi-well cap technique (Psychoyos et al., 1991), transwell tissue culture plates (Smart and Casale, 1993), and the use of non-disposable chemotaxis chambers. Non-disposable chemotaxis chambers have been adapted to a variety of multi-well formats including 48-well and 96-well formats. An advantage of the 48-well and 96-well formats is that they offer the ability to make multiple comparisons within a single chemotaxis chamber. While the general design of the 48-well and 96-well non-disposable chemotaxis chambers is similar, parameters such as upper and lower well volumes vary. Furthermore, parameters such as incubation time, cell numbers, filter pore size, and filter composition vary in published studies.

One major difference between the 48-well and 96-well non-disposable chemotaxis chambers is the methods used to measure leukocyte migration. Leukocyte migration in the 48-well format is usually measured by identifying and counting the number of cells that are in the filter either visually (Goodman et al., 1991) or with an image analysis system (Harvath et al., 1994, 1980; Leonard et al., 1991). A potential problem with counting cells visually is that this procedure is labor intensive and can lead to delays in obtaining data. In addition, counting cells visually is often subjective.

Several different techniques have been described to measure leukocyte migration in 96-well chemotaxis chambers. While one can still count cells visually in or on the 96-well filter, investigators have used cellular markers such as the fluorescent probe, BCECF-AM (DeForge et al., 1992), peroxidase content (Junger et al., 1993), or the reduction of 3-(4,5-dimethylthiazol-2-yl)-2,5-diphenol tetrazolium bromide (MTT) (Shi et al., 1993) to estimate cell numbers. Changes in intracellular pH following PMN activation have been shown to cause a decrease in total fluorescence of activated PMN labeled with the pH sensitive fluorescein derivative, BCECF-AM (Frevert et al., 1994; Vaporciyan et al., 1993). A decrease in the total fluorescence of activated PMN could result in an underestimate of PMN migration. A disadvantage of using MTT reduction or peroxidase content is that these techniques require large volumes of chemoattractant in the lower wells of the assay (i.e., 200–400 μl). The use of low volume plates (i.e., 30 μl/well) for the MTT and peroxidase assay has not been reported. The total volume used in the lower wells of the chamber is important when the chemoattractant is expensive or limited in quantity.

We now report studies with a new disposable 96-well chemotaxis chamber (ChemoTx, Neuro Probe, Gaithersburg, MD) that permits rapid and consistent measurement of PMN migration in vitro using calcein AM-labeled PMN in low volume plates (30 μl/well). We evaluated the technical parameters that affect the assay, including cell density, filter pore size, membrane composition, and thickness. In addition, we compared PMN migration in the new disposable 96-well chamber using total fluorescence as a cellular marker of PMN migration (i.e., fluorescence end-point assay) with chemotaxis performed in a 48-well chamber where PMN migration was measured by visually counting cells (i.e., visual end-point assay). As compared with the visual end-point assay, the fluorescence end-point assay is more rapid and more sensitive. This new system is a significant advance over traditional assays for measuring leukocyte migration.

2. Materials and methods

2.1. Preparation of leukocytes

Heparinized whole blood (20–30 ml) was collected from healthy human donors, layered over a density gradient (mono–poly resolving media, ICN Pharmaceuticals, Costa Mesa, CA) and spun at $400 \times g$ for 30 min. The PMN rich fraction was removed and if necessary, RBC were lysed with hypotonic saline. The PMN were washed twice with pyrogen-free phosphate buffered saline (PBS) (Sigma, St. Louis, MO) and then resuspended

in 5.0 ml RPMI-1640 without phenol red (BioWhittaker, Walkersville, MD) containing 10% heat-treated fetal calf serum (RPMI-FCS) (HyClone, Logan, UT).

Calcein AM (Molecular Probes, Eugene, OR) (5 μg/ml) was added to the 5.0 ml suspension of cells in RPMI-FCS and the cells were incubated for 30 min at 37°C (Quan et al., 1996). Neutrophils were washed twice with PBS, counted and resuspended in RPMI-FCS to the desired concentration.

2.2. Reagents

Chemotactic factors were diluted to 1×10^{-5} M in PBS containing 0.1% pyrogen-free human serum albumin (PBS-HSA) and aliquots were stored at −70°C. The C–X–C chemokine, interleukin-8 (PeproTech, Rocky Hill, NJ), and the complement fragment, C5a (Sigma), were purchased as recombinant human peptides. On the day of each experiment, aliquots were diluted in PBS with 0.1% human serum albumin (PBS-HSA) or PBS with 100 μg/ml cytochrome *c* (Sigma) to the final concentrations indicated. Zymosan activated serum (ZAS) was also used as a chemotactic factor. Zymosan activated serum was prepared from normal human serum as described (Pillemer et al., 1956). Phorbol myristate acetate (PMA) was diluted to 5 μg/ml in DMSO and aliquots were stored at −70°C. PMA was used at a final concentration of 50 ng/ml in PBS-HSA.

2.3. Measurement of PMN migration

2.3.1. Determination of PMN migration using the visual end-point assay

We used two established protocols for the measurement of PMN migration using the 48-well chemotaxis chamber with a visual end-point assay (Neuro Probe). The first set of experiments in the 48-well chamber used nitrocellulose filters (Goodman et al., 1991), the second set of experiments used polycarbonate filters (Harvath et al., 1994; Leonard et al., 1991).

Migration was measured using 48-well chambers with nitrocellulose filters using methods previously described (Goodman et al., 1991). Briefly, dilutions of chemotactic factors were made in PBS and added to the bottom wells (25 μl) of the 48-well plate. Nitrocellulose filters (Neuro Probe) with a 3 μm pore size were placed between the bottom plate and top plate of the chamber assembly and the PMN (60 μl) were added to the top wells at a cell density of 3×10^6 PMN/ml. The chamber was incubated for 1.5 h (37°C and 5% CO_2) and the non-migrating cells on the origin side (i.e., top) of the filter were removed by gentle scraping. The filter was dried, fixed and stained with a modified hematoxylin/eosin stain. Filters were mounted on glass slides and PMN migration was measured visually by counting the number of cells at the leading front of migration in 10 high-powered fields (×450).

Migration was measured using 48-well chambers with PVP free polycarbonate filters as previously described (Harvath et al., 1994; Leonard et al., 1991). Briefly, dilutions of chemotactic factors were made in PBS with 100 μg/ml cytochrome *c* (Sigma) and added to the bottom wells (25 μl) of the 48-well plate. PVP free polycarbonate filters (Neuro Probe) with 5 μm pore size were placed between the bottom plate and top plate of the chamber assembly and the PMN (45 μl) at a concentration of 1×10^6 PMN/ml were added to the top wells. The chamber was incubated for 40 min (37°C and 5% CO_2) and the non-migrating cells on the origin side (i.e., top) of the filter were removed by gentle scraping. The filter was dried, fixed and stained with a Diff-Quik stain (Baxter Health Care, McGaw Park, IL). Filters were mounted on glass slides and PMN migration was measured visually by counting the number of PMN in five high-powered fields (×450).

2.3.2. Fluorescence-based determination of PMN migration (fluorescence end-point assay)

The new disposable 96-well chemotaxis chamber (ChemoTx, Neuro Probe) used for these studies differs from the previous design for the non-disposable 48-well chamber and non-disposable 96-well chamber (Fig. 1A and B). The major design change is that the filter has a hydrophobic mask surrounding each of the 96 filter sites (Fig. 1B). The filter sites on the new 96-well filter are 3.2 mm in diameter yielding a filter area of 8 mm^2 per

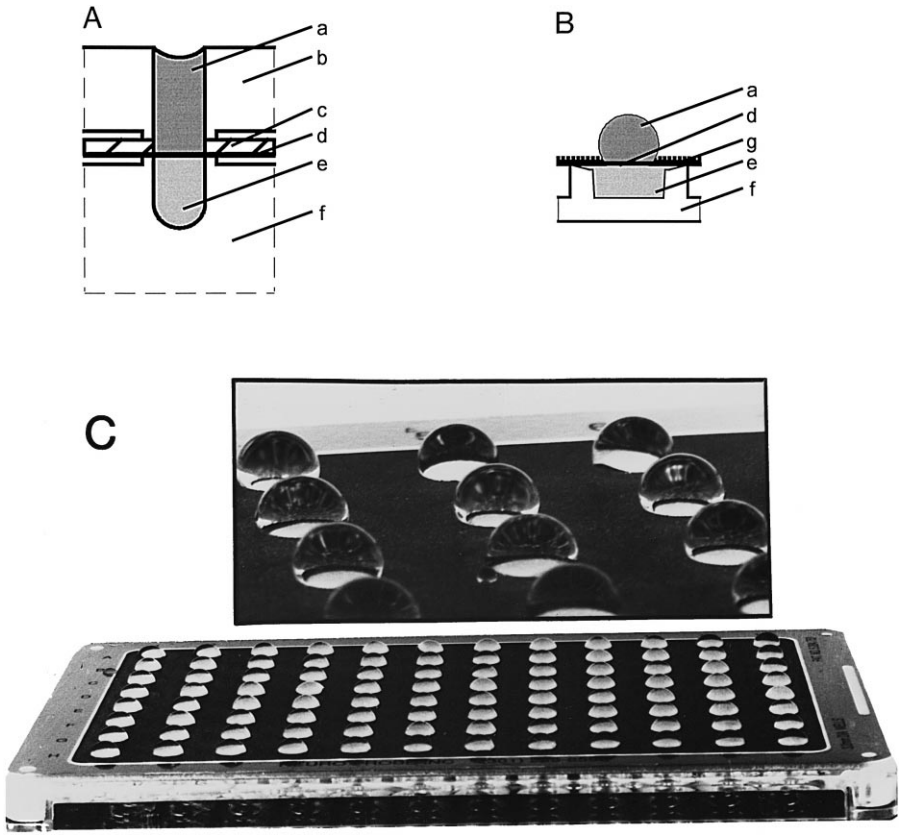

Fig. 1. Cross-section (scale 4:1) of one well of (A) the 48-well non-disposable and 96-well non-disposable chemotaxis chamber and (B) the new disposable 96-well chemotaxis chamber. (a) Cell suspension, (b) upper chamber, (c) silicon gasket, (d) filter, (e) chemotactic factor, (f) lower chamber, (g) hydrophobic mask. (C) Photograph of the new disposable 96-well chemotaxis chamber. The higher magnification insert shows the cell suspensions on top of the filter held in place by the black hydrophobic mask.

site, which is the same size as the filter sites for the 48-well chamber. The new filter used in the disposable 96-well format eliminates the need for a top chamber, because the hydrophobic mask around each filter site creates surface tension in the cell suspension, which keeps it positioned on the hydrophilic filter site located directly above the bottom wells (Fig. 1C).

To set up the 96-well chamber, the wells in the microplate (e.g., bottom chamber) were filled with 29 μl of chemotactic factors diluted in PBS-HSA or the negative control (i.e., PBS-HSA). In order to determine the total fluorescence of the PMN added to the origin side of the filter, 25 μl of each cell suspension (i.e., 0.25, 0.5, 1.0, 2.0, 3.0, and 5.0×10^6 PMN/ml) was placed directly in three wells in the bottom chamber. The polycarbonate or polyester filters (Table 1) were positioned on the loaded microplate and secured in place with corner pins. Neutrophils (25 μl) were placed directly onto the filter sites and the chamber was incubated for 1 h (37°C and 5% CO_2). The non-migrating cells on the origin side (i.e., top) of the filter were removed by gently wiping the filter with a tissue. The chemotaxis chamber was placed in a multi-well fluorescent plate reader (CytoFluor II, PerSeptive Biosystems, Framingham, MA) and the cells that migrated into the bottom chamber were measured by using the calcein fluorescence signal. The fluorescent plate reader was configured so that the probe was in a bottom-read position, which allowed for the detection of fluorescence in each well of the chemotaxis chamber (excitation, 485 nm; emission, 530 nm).

Table 1
Characteristics of the chemotaxis filters

Filter material	Pore size (μm)	Pores/well	Thickness (μm)
Thin polycarbonate filter	3	160,000	9
	5	32,000	10
	8	8000	7
Thick polycarbonate filter	3	160,000	15
	5	32,000	17
	8	8000	12
Thick polyester filter	3	160,000	20
	5	32,000	18
	8	8000	15

2.4. Data analysis

To determine if there was a linear association between total fluorescence and the number of PMN, statistical analysis was performed using the Pearson correlation coefficient of correlation (Milton et al., 1983). All values are expressed as means and standard error (SE).

PMN migration towards each chemotactic factor was expressed as the raw data, which are the cell counts per 5 or 10 hpf for the visual end-point assays and the total fluorescence for each well of the 96-well plate for the fluorescence end-point assay. In order to minimize day-to-day and donor-to-donor variability, data from the fluorescence end-point assay was also expressed as the % total PMN. The % total PMN is determined using three variables. The first variable is the total fluorescence of the well of interest. The second variable is the mean total fluorescence of the negative control wells that contain PBS-HSA. The third variable is the mean total fluorescence of 25 μl of the calcein AM-labeled PMN placed directly into the bottom chamber to determine the fluorescence of the total number of cells added (total PMN).

$$\%\,\text{Total PMN} = 100 \times \frac{\text{mean total fluorescence in wells of interest} - \text{mean total fluorescence of PBS wells}}{\text{mean total fluorescence of total PMN}}$$

The ratio of directed migration to random migration (D/R ratio) was determined to define whether a certain cell density or pore size offered a significant advantage. The D/R ratio was calculated by dividing the mean fluorescence of PMN that migrated toward an individual chemotactic factor (e.g., ZAS or IL-8) by the mean fluorescence of random PMN migration to PBS-HSA.

$$\text{D/R} = \frac{\text{total fluorescence of wells containing chemoattractant}}{\text{total fluorescence of wells containing PBS}}$$

In order to compare the variability among a group of wells, the coefficient of variation (CV) was also determined as follows (Milton and Tsokos, 1983):

$$\text{CV} = \frac{\sigma s}{\text{FS}} \times 100$$

Where: fluorescent signal (FS) = mean total fluorescence of wells of interest − mean total fluorescence of wells containing PBS; $\sigma s = [(\sigma\ \text{Wells of interest})^2 + (\sigma\ \text{Wells containing PBS})^2]^{1/2}$.

3. Results

3.1. Evaluation of the calcein signal in PMN

Because the activation of PMN had been shown to cause a decreased fluorescence of BCECF-AM loaded PMN (Frevert et al., 1994; Vaporciyan et al., 1993), PMN were treated with three agonists (i.e., IL-8, C5a, and

Table 2
Effect of stimulation of calcein-labeled PMN on mean cellular fluorescence

Treatment	TF
Untreated cells (i.e., PBS)	27,102 (±3927)
IL-8 (1×10^{-7} M)	28,049 (±3023)
C5a (1×10^{-7} M)	27,502 (±3094)
PMA [50 ng/ml]	25,517 (±3312)

TF = total fluorescence of calcein-labeled PMN (3×10^5) incubated for 30 min with the indicated agonists.

PMA) for 30 min to determine whether activation would alter the fluorescence of calcein AM-labeled PMN. Treatment of calcein AM-labeled PMN with IL-8 (1×10^{-7} M), C5a (1×10^{-7} M) or PMA (50 ng/ml) did not significantly change the fluorescence signal when compared with PMN treated with PBS (i.e., untreated control) (Table 2).

To determine if there was a linear relationship between cell number and the fluorescence signal, PMN were labeled with calcein AM, then diluted serially (10 PMN to 3×10^6 PMN/well) and fluorescence was measured in the fluorescence plate reader in triplicate. The relationship between cell number (100 to 300,000 PMN/well) and total fluorescence was linear ($r = 0.9891$, $p < 0.000001$) and the lower limit of detection was approximately 75 PMN/well (Fig. 2).

3.2. Effect of cell density and pore size on PMN migration

We evaluated the effects of cell density and filter pore size on PMN migration using two different agonists (i.e., ZAS and IL-8). Neither pore size nor cell density affected the migration of PMN toward IL-8 (1×10^{-7} M) or ZAS (1:10 dilution). In fact, when PMN migration was measured with varying conditions of pore size and cell density, nearly all the PMN migrated when IL-8 (1×10^{-7} M) or ZAS (1:10 dilution) were placed in the bottom wells (Fig. 3A and B). We also found that the pore size did not influence PMN migration toward three different concentrations of IL-8 using 3×10^6 PMN/ml (Fig. 4). Although neither pore size nor cell concentration affected PMN migration towards IL-8 and ZAS, pore size did affect random migration towards the negative control (i.e., PBS-HSA) (Fig. 3C). There was a trend toward more random migration in the 3 μm filters as compared with the 5 μm or 8 μm filters.

To optimize the fluorescence end-point assay for pore size and cell density, the D/R ratio and CV were calculated for filters of three different pore sizes (i.e., 3, 5, and 8 μm) and for several different concentrations of PMN. While there were no significant differences in the D/R ratio for the three pore sizes, (i.e., 3, 5 and 8 μm) there was a trend for a higher D/R ratio for the 8 μm filter when 1×10^6, 3×10^6, and 5×10^6

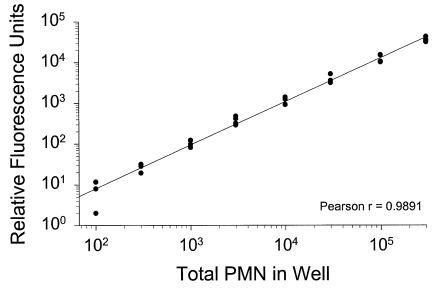

Fig. 2. The relationship between cell numbers (100 to 3×10^5 PMN) and fluorescence expressed as relative fluorescence units. Each symbol represents the relative fluorescence per well at each concentration of PMN in one experiment ($n = 4$). The relationship between cell number and total fluorescence per well was linear ($r = 0.9891$, $p < 0.00001$).

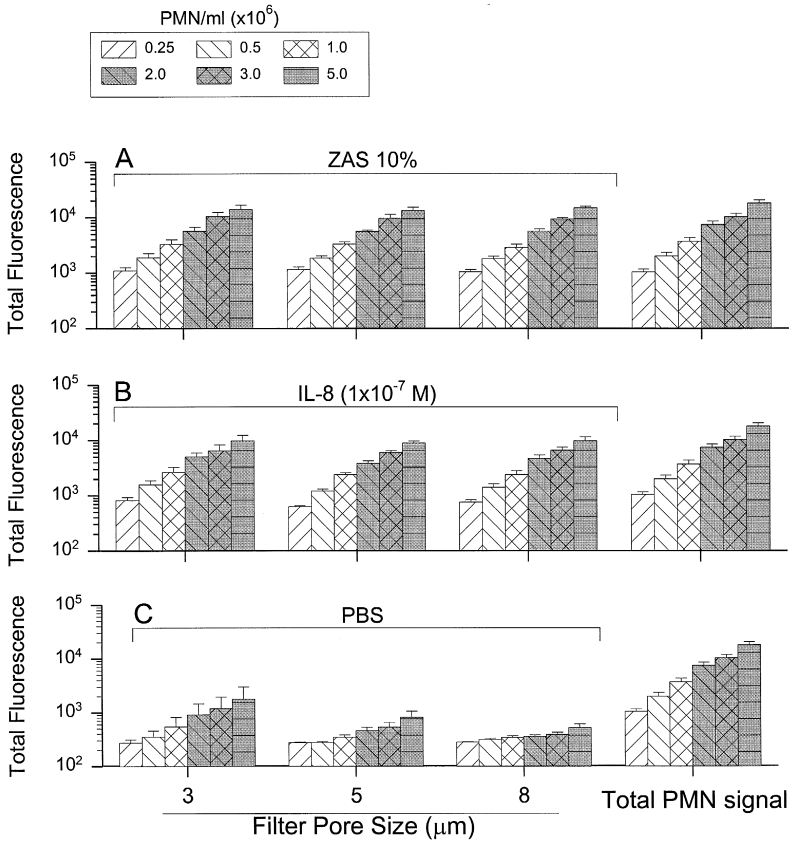

Fig. 3. Effect of PMN concentration and filter pore size on PMN migration. Neutrophil migration was measured towards (A) zymosan activated serum (ZAS), (B) IL-8, and (C) phosphate buffered saline (PBS). To determine the total number of PMN that could migrate in each assay, the cell suspension was placed directly into the bottom chamber of additional wells and the fluorescence was measured at the end of the study (total PMN signal). The pore size did not influence PMN migration toward the chemotactic peptides ZAS or IL-8 (Panels A and B) but the pore size influenced the random migration (Panel C). The values are the means + SE of assays performed using PMN isolated from three volunteers ($n = 3$).

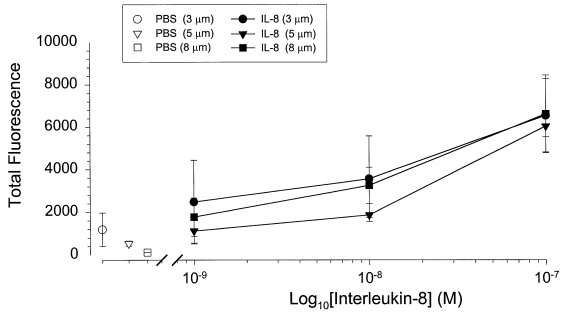

Fig. 4. Filter pore size (i.e., 3, 5, and 8 μm pores) did not affect PMN migration to IL-8. Direct comparisons of PMN migration (3×10^6 PMN/ml which is 7.5×10^4 PMN/well) through polycarbonate filters of varying pore size. The data represent three experiments using PMN collected from three volunteers ($n = 3$). The values are the means + SE.

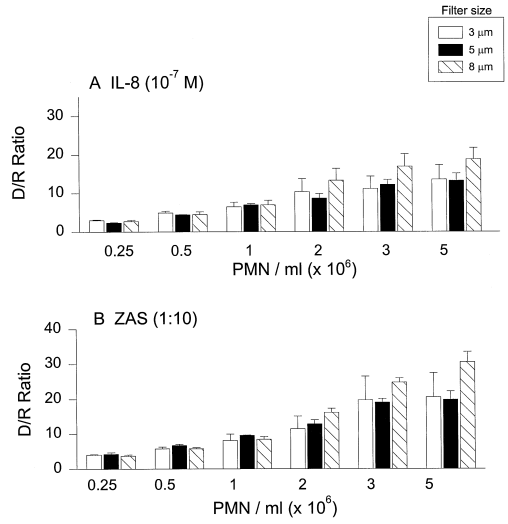

Fig. 5. The ratio of directed migration to random migration (D/R ratio) in the fluorescence end-point assay comparing cell number and pore size. The D/R ratio was determined from PMN migrating towards (A) interleukin-8 or (B) 10% ZAS. The D/R ratio was calculated as described (Section 2). The values are the means + SE.

PMN/ml were used in this assay (Fig. 5A and B). When the CV for each pore size and cell density was determined, the 8 μm filter consistently had a lower CV (Table 3). Based on the finding that the 8 μm pore size consistently had the highest D/R ratio and lowest CV, we chose to use this filter for the studies described. We also chose to use 3×10^6 PMN/ml (i.e., 75,000 PMN/well) because this concentration gave a high D/R ratio and permitted as many as four 96-well chemotaxis chambers assays to be used with the PMN received from 30 ml of blood from a single donor.

3.3. Comparison of different filters

To determine whether filter composition (polycarbonate vs. polyester) or filter thickness (7 μm vs. 15 μm) affected PMN migration, we compared the ability of PMN to migrate toward IL-8 and C5a using three different

Table 3
Determination of the coefficient of variation (CV) for IL-8

Pore size (μm)	2.5×10^5 PMN/ml	5.0×10^5 PMN/ml	1.0×10^6 PMN/ml	2.0×10^6 PMN/ml	3.0×10^6 PMN/ml	5.0×10^6 PMN/ml
CV for IL-8 at 1×10^{-7} M						
3	5 (+1)	11 (+1)	15 (+9)	13 (+7)	6 (+2)	20 (+13)
5	34 (+25)	18 (+12)	16 (+6)	32 (+17)	16 (+4)	15 (+7)
8	9 (+3)	8 (+2)	13 (+3)	18 (+8)	15 (+5)	28 (+16)
CV for IL-8 at 1×10^{-8} M						
3	23 (+1)	23 (+18)	50 (+41)	56 (+48)	59 (+43)	20 (+220)
5	88 (+25)	48 (+26)	38 (+20)	37 (+13)	53 (+15)	15 (+13)
8	16 (+3)	9 (+3)	14 (+3)	15 (+6)	11 (+3)	28 (+7)
CV for IL-8 at 1×10^{-9} M						
3	14 (+3)	76 (+53)	39 (+19)	235 (+209)	78 (+58)	216 (+197)
5	156 (+117)	46 (+24)	37 (+14)	38 (+20)	90 (+67)	46 (+21)
8	111 (+94)	42 (+30)	20 (+5)	28 (+13)	21 (+9)	21 (+11)

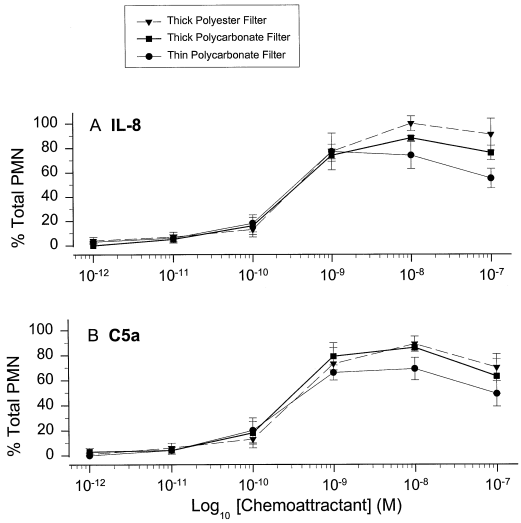

Fig. 6. Direct comparison of PMN migration through the 8 μm thin polycarbonate filter, the 8 μm thick polycarbonate filter and the 8 μm thick polyester filter. Neither filter composition nor filter thickness affected PMN migration toward IL-8 (A) and C5a (B). The values are the means + SE of assays performed using PMN isolated from three volunteers ($n = 3$).

filters (Table 1). All of the filters had a pore size of 8 μm, and PMN were used at a concentration of 3.0×10^6 PMN/ml (i.e., 75,000 PMN/well). Neither filter composition nor filter thickness affected PMN migration toward IL-8 or C5a (Fig. 6).

3.4. Comparison of the visual end-point assay with the fluorescence end-point assay

Direct comparisons were made between the visual end-point assay and the new fluorescence end-point assay. These comparisons were made on the same day using PMN collected from a single individual. In the first set of experiments, we made a direct comparison between the fluorescence end-point assay and a visual end-point assay using nitrocellulose filters (Fig. 7). In a second set of experiments, we compared the fluorescence

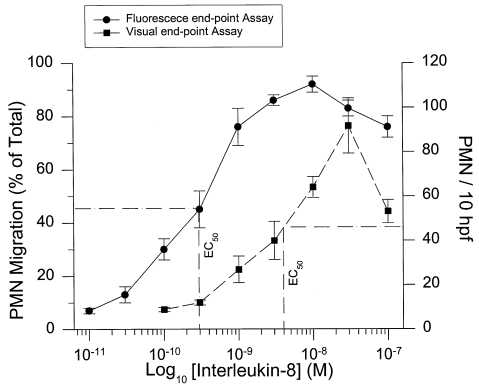

Fig. 7. Direct comparison of PMN migration toward IL-8 using the visual end-point (nitrocellulose filters with 3 μm pores) and fluorescence end-point assay (polycarbonate filters with 8 μm pores). The data are shown as the percentage of total cells migrating in the fluorescence end-point assay (left vertical axis), and PMN per 10 high-powered fields for the visual end-point assay (right vertical axis). Based on their respective EC_{50}, the fluorescence end-point assay is 10 times more sensitive than the visual end-point assay. The values are the means + SE of assays performed using PMN isolated from three volunteers ($n = 3$).

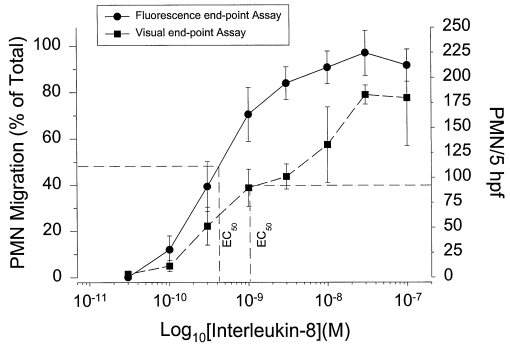

Fig. 8. Direct comparison of PMN migration toward IL-8 using the visual end-point (polycarbonate filters with 5 μm pores) and the fluorescence end-point assay (polycarbonate filters with 8 μm pores). The data are shown as the percentage of total cells migrating in the fluorescence end-point assay (left vertical axis) and PMN per five high-powered fields in the visual end-point assay (right vertical axis). Based on their respective EC_{50}, the fluorescence end-point assay is 2.5 times more sensitive than the visual end-point assay. The values are the means + SE of assays performed using PMN isolated from three volunteers ($n = 3$).

end-point assay with a visual end-point assay using polycarbonate filters (Fig. 8). In all comparisons, we found that the peak PMN signal was similar (Figs. 7 and 8). However, the fluorescence end-point assay was more sensitive, as the effective concentration for 50% maximal chemotaxis (EC_{50}) was at least 10-fold lower in the fluorescence end-point assay as compared with the visual assay when nitrocellulose filters were used (Fig. 7). When polycarbonate filters were used in the visual end-point assay, the EC_{50} for the fluorescence end-point assay was 2.5-fold lower than the visual end-point assay (Fig. 8).

4. Discussion

We have systematically evaluated the operating characteristics of a new 96-well fluorescence end-point assay used for the measurement of PMN migration in vitro. The results indicate that the new fluorescence end-point assay is rapid and reproducible, and is not affected by filter pore size, cell density, filter composition, or filter thickness. We also found this assay to be sensitive at low concentrations of cells and chemoattractants. When compared with the visual end-point assay, we found that the fluorescence end-point assay was less labor intensive, more rapid, and more sensitive.

BCECF-AM has been used as a fluorescent label for measurement of PMN migration in prior studies (DeForge et al., 1992; Frevert et al., 1995, 1994). One potential problem with the use of BCECF-AM labeled PMN is that their fluorescence intensity changes when PMN are activated (Frevert et al., 1994). The change in fluorescence intensity of BCECF-AM labeled PMN with activation is probably a consequence of the pH-dependent emission spectra of this fluorescein derivative (Haugland, 1996). Calcein, which is the hydrolysis product of calcein AM, is a fluorescent probe related to fluorescein that labels viable cells and is pH insensitive. To show that PMN activation did not affect the fluorescence of calcein AM-labeled PMN, we treated these cells with three agonists (i.e., PMA, IL-8 and C5a) and compared their mean fluorescence with PMN treated with the vehicle (i.e., PBS). None of the agonists used in this study altered the fluorescence signal of calcein AM-treated PMN (Table 2). We also found that the calcein AM labeling did not affect the migration of PMN in the visual end-point assay (not shown). Calcein was a sensitive label because as few as 75 PMN/well could be detected and there was a linear relationship between total fluorescence and cell number when 100 to 300,000 PMN/well were evaluated (Fig. 2).

A previous study had shown that PMN migration toward IL-8 was influenced by the pore size in the

polycarbonate filters used in a visual end-point assay (Rot, 1991). We therefore evaluated the affect of pore size and cell concentration on PMN migration towards both IL-8 and ZAS. Neither pore size nor cell concentration affected PMN migration to either IL-8 or ZAS in the fluorescence end-point assay (Figs. 3 and 4). We did, however, see a trend towards higher random migration when using the 3 μm filters (Fig. 3C). One possible explanation for an increase in random migration in these filters is that there are more pores per well in the 3 μm filters as compared with either the 5 or 8 μm filters (Table 1).

The influence of filter composition and thickness was also evaluated to determine if either of these parameters would modify PMN migration. In this study, a thick polyester filter, thick polycarbonate filter and a thin polycarbonate filter all with an 8 μm pore size were used (Table 1). Neither filter thickness nor filter composition appeared to influence PMN migration toward IL-8 or C5a (Fig. 6). This finding is important because it means that one can use filters of varying composition and thickness and still obtain similar results when measuring PMN migration in vitro with the fluorescence end-point assay.

Direct comparisons were made between the standard visual end-point assay and the fluorescence end-point assay. The time required to set up the two assays was similar. A major improvement in the setup in the new disposable 96-well chemotaxis chamber is the development of a hydrophobic mask on the top of the filter that allows for the placement of the cell suspension directly on top of the filter without an upper chamber (Fig. 1). Two common problems of non-disposable chemotaxis chambers, pipetting errors and bubble entrapment, are solved by this improvement. While setup time for the two chambers was similar, the visual-based determination of PMN migration was more labor intensive because the data were acquired using a light microscope to visually count the number of PMN in 5–10 hpf for each well. Typically, it will take an experienced person 2 to 3 h to count one filter from a 48-well chamber. If filters from the 48-well chamber are counted using an image analysis system the time to count a 48-well filter can be reduced to 30 min. In contrast, the fluorescence-based determination of PMN migration allows rapid acquisition (i.e., 5 min for a 96-well plate) and analysis of the data. Another advantage of the fluorescence end-point assay is that data acquisition is objective, whereas the visual end-point assay has the potential for operator bias.

When the sensitivities of the visual end-point and fluorescence end-point assay were compared, we found that the new fluorescence end-point assay was up to 10 times more sensitive than the visual end-point assay (Figs. 7 and 8). The increased sensitivity in the fluorescence end-point assay probably results from the different methods used to measure PMN migration in the two assays. In the visual end-point assay, PMN migration is measured by counting only the number of PMN in or adherent to the bottom of the filter. In contrast, the fluorescence end-point assay measures the PMN in the filter, PMN that are adherent to the bottom of the filter and those that have dropped off the filter and have migrated into the lower chamber of the chemotaxis assay. A potential problem with only counting the PMN in or on the filter, in the visual end-point assay, is that cells may drop off the filter into the lower chamber, resulting in an underestimate of PMN migration (Harvath et al., 1980; Leonard et al., 1991).

In addition to total fluorescence, the data for the fluorescence end-point assay also were expressed as the % of total PMN (Figs. 7 and 8). The expression of the data as the % of total PMN did not change the chemotactic profile for PMN migration towards either IL-8 or C5a (data not shown). One advantage that the conversion of the raw data (i.e., total fluorescence) to % total PMN offers is that it minimizes the day-to-day variability in calcein AM-loading of PMN. While the unequal loading of calcein by PMN does not influence PMN migration and the chemotactic profile obtained with the assay, it does increase the variability of the assay when comparisons are made on different days.

In conclusion, the fluorescent-quantitation of PMN migration is a sensitive, convenient, and reliable assay for the measurement of PMN migration in vitro. The fluorescence end-point assay is technically superior to the 48-well visual end-point assay, as it is less labor-intensive, allows for the rapid acquisition and analysis of data, has no operator bias and is 2.5 to 10 times more sensitive. The 96-well format also allows for multiple comparisons to be made under identical conditions. Therefore, this fluorescence end-point assay is a significant improvement over existing methods and is ideal for the initial characterization of chemotactic factors.

Acknowledgements

The authors thank Kristine Wynant, Nancy Welch and Mark Phillips for their help in the preparation of the manuscript. Supported in part by NIH Grants AI29103, HL30542, HL51072, the American Lung Association of Washington, and the Medical Research Service of the Department of Veterans Affairs.

References

DeForge, L.E., Kenney, J.S., Jones, M.L., Warren, J.S., Remick, D.G., 1992. Biphasic production of IL-8 in lipopolysaccharide (LPS)-stimulated human whole blood. Separation of LPS- and cytokine-stimulated components using anti-tumor necrosis factor and anti-IL-1 antibodies. J. Immunol. 148, 2133.

Frevert, C.W., Warner, A.E., Kobzik, L., 1994. Defective pulmonary recruitment of neutrophils in a rat model of endotoxemia. Am. J. Respir. Cell. Mol. Biol. 11, 716.

Frevert, C.W., Huang, S., Danaee, H., Paulauskis, J.D., Kobzik, L., 1995. Functional characterization of the rat chemokine KC and its importance in neutrophil recruitment in a rat model of pulmonary inflammation. J. Immunol. 154, 335.

Goodman, R.B., Forstrom, J.W., Osborn, S.G., Chi, E.Y., Martin, T.R., 1991. Identification of two neutrophil chemotactic peptides produced by porcine alveolar macrophages. J. Biol. Chem. 266, 8455.

Haddox, J.L., Knowles, I.W., Sommers, C.I., Pfister, R.R., 1994. Characterization of chemical gradients in the collagen gel-visual chemotactic assay. J. Immunol. Meth. 171, 1.

Harvath, L., Falk, W., Leonard, E.J., 1980. Rapid quantitation of neutrophil chemotaxis: use of a polyvinylpyrrolidone-free polycarbonate membrane in a multi-well assembly. J. Immunol. Meth. 37, 39.

Harvath, L., Brownsom, N.E., Fields, G.B., Skubitz, A.P.N., 1994. Laminin peptides stimulate human neutrophil motility. J. Immunol. 152, 5447.

Haugland, R., 1996. pH indicators. In Handbook of Fluorescent Probes and Research Chemicals. Molecular Probes, p. 551.

Junger, W.G., Cardoza, T.A., Liu, F.C., Hoyt, D.B., Goodwin, R., 1993. Improved rapid photometric assay for quantitative measurement of PMN migration. J. Immunol. Meth. 160, 73.

Krauss, A.H., Nieves, A.L., Spada, C.S., Woodward, D.F., 1994. Determination of leukotriene effects on human neutrophil chemotaxis in vitro by differential assessment of cell motility and polarity. J. Leukocyte Biol. 55, 201.

Leonard, E.J., Yoshimura, T., Rot, A., Noer, K., Walz, A., Baggiolini, M., Walz-D, A., Goetzl, E.J., Castor, C.W., 1991. Chemotactic activity and receptor binding of neutrophil attractant/activation protein-1 (NAP-1) and structurally related host defense cytokines: interaction of NAP-2 with the NAP-1 receptor. J. Leukocyte Biol. 49, 258.

Milton, J.S., Tsokos, J.O., 1983. Statistical Methods in the Biological and Health Sciences. McGraw-Hill, New York, NY.

Milton et al., 1983.

Pillemer, L., Blum, L., Lepow, I., Wurz, L., Todd, E.W., 1956. Properdin system and immunity: zymosan assay of properdin. J. Exp. Med. 103, 1.

Psychoyos, S., Uziel-Fusi, S., Morrissey, M., Ganu, V., Smith, C., 1991. Thick filter neutrophil chemotaxis performed in the absence of albumin. J. Immunol. Meth. 137, 37.

Quan, J.M., Martin, T.R., Rosenberg, G.B., Foster, D.C., Whitmore, T., Goodman, R.B., 1996. Antibodies against the N-terminus of IL-8 receptor A inhibit neutrophil chemotaxis. Biochem. Biophys. Res. Commun. 219, 405.

Rot, A., 1991. Chemotactic potency of recombinant human neutrophil attractant/activation protein-1 (interleukin-8) for polymorphonuclear leukocytes of different species. Cytokine 3, 21.

Shi, Y., Kornovski, B.S., Savani, R., Turley, E.A., 1993. A rapid, multi-well colorimetric assay for chemotaxis. J. Immunol. Meth. 164, 149.

Smart, S.J., Casale, T.B., 1993. Interleukin-8-induced transcellular neutrophil migration is facilitated by endothelial and pulmonary epithelial cells. Am. J. Respir. Cell. Mol. Biol. 9, 489.

Vaporciyan, A.A., Jones, M.L., Ward, P.A., 1993. Rapid analysis of leukocyte-endothelial adhesion. J. Immunol. Meth. 159, 93.

Zicha, D., Dunn, G.A., Brown, A.F., 1991. A new direct-viewing chemotaxis chamber. J. Cell Sci. 99, 769.

Zigmond, S.H., 1977. Ability of polymorphonuclear leukocytes to orient in gradients of chemotactic factors. J. Cell Biol. 75, 606.